

Semi-Annual Report  
July - December 1994

Michael D. King and Si-Chee Tsay  
Goddard Space Flight Center  
Greenbelt, MD 20771

**Abstract**

Our major achievements of the past six months are threefold: (1) extensive study of MAS calibration to establish proper procedures, (2) analyses of ASTEX data using MAS remote sensing/retrievals and *in situ* microphysical data, and (3) analyses of MAS data to study the effects of ship effluents on cloud properties.

**I. Task Objectives**

With the use of related airborne instrumentation, such as the MODIS Airborne Simulator (MAS) and Cloud Absorption Radiometer (CAR) in intensive field experiments, our primary objective is to extend and expand algorithms for retrieving the optical thickness and effective radius of clouds from radiation measurements to be obtained from the Moderate Resolution Imaging Spectroradiometer (MODIS). The secondary objective is to obtain an enhanced knowledge of surface angular and spectral properties that can be inferred from airborne directional radiance measurements.

**II. Work Accomplished**

*a. MODIS-related Algorithm Study*

The revision (version 3) of the MODIS Algorithm Theoretical Basis Document (ATBD) was completed by Michael King, Si-Chee Tsay, Steven Platnick, and Menghua Wang and delivered to the EOS Project Science Office in time. The title of this ATBD was changed to "Cloud Retrieval Algorithms for MODIS: Optical Thickness, Effective Particle Radius and Thermodynamic Phase" to reflect the treatment of cloud masking as a separate product and to respond to reviewers' comments. The initial MODIS -II software (cloud retrieval algorithms) was delivered by Menghua Wang to the MODIS Science Data Support Team (SDST). This package includes eight new lookup tables (4 for the reflection functions, 3 for the flux parameters, and 1 for the asymptotic parameters) and one cloud retrieval code with input test data and expected outputs.

*b. MODIS-related Instrumental Research*

During the past six months, we have spent a considerable amount of time and effort on MAS calibration, including radiometric calibration and spectral characterization. Radiometric calibration of the visible and near-infrared channels is obtained by observing laboratory standard integrating sphere sources on the

ground before and after flight missions, while calibration of the infrared channels is accomplished by viewing two onboard blackbody sources that are viewed once every scan. A summary (flowchart) of the calibration and temperature correction procedure involving visible and near-infrared channels is shown in Fig. 1 and discussed in detail below.

The most important issue in radiometric calibration is obtaining and using a suitable and stable source, such as an integrating hemisphere or integrating sphere. Previously, the NASA Goddard 48-inch integrating hemisphere was the standard for MAS radiometric calibration. Data for different gain settings were acquired using the Ames 20-inch integrating hemisphere and 30-inch sphere sources, and the radiance values for the Ames 30-inch sphere and Goddard 48-inch hemisphere sources were compared using John Cooper's laboratory calibrations. Optronics data for independent calibrations were also used. The radiance/count values were computed for data from all three sources using John Cooper's radiance values as well as using Optronics radiance values (only for the 30-inch source). For all calibrations conducted for each calibration source, MAS raw counts for each channel were extracted and linearly regressed with appropriate source radiance values. This produced for each source a gain (radiance/raw count) value for each MAS channel. Figure 2 compares the Goddard 48-inch hemisphere and Ames 30-inch sphere with Ames 20-inch hemisphere for relative difference in gain change. Note that very good agreement for the 48 and 20-inch sources ( $< 5\%$ ) is achieved, and relatively good agreement (except for the  $1.88\ \mu\text{m}$  water vapor channel) with the 20 and 30-inch data.

Distance tests were also performed to verify if the Ames 20-inch integrating hemisphere (purchased for its portability to ship wherever the MAS goes) is suitable for absolute MAS radiometric calibration. The BOREAS mission (see below) was the first deployment of the MAS onboard the NASA C-130 aircraft. Prior to each flight, radiance measurements of the Ames 20-inch hemisphere were recorded by the MAS, in which the 20-inch hemisphere was placed very close to the MAS (as was necessary due to the location of the instrument under the fuselage of the aircraft only 2 feet above the ground). It was found that radiance values for the 20-inch hemisphere were a strong function of distance between the MAS instrument and the hemisphere. Results are summarized in Table 1 below. The sensitivity of the calibration with distance from the source is important because it means that the MAS must be removed from the aircraft pod to be absolutely calibrated. In each daily mission a pre-flight calibration of the MAS was obtained, with the instrument remaining in the pod and the hemisphere rolled under it about 2" away. As a result, these pre-flight calibration tests were useful only as a relative calibration check during deployment.

Another investigation of MAS radiometric calibration was conducted using differences in the 20-inch hemisphere when operated at 2 slightly different current levels (at 2.78 and 2.8 volts). John Cooper calibrated the hemisphere mostly at 2.8 volts but occasionally at 2.78 volts (5, 3, and 2 lamps). Analyses of the 20-inch

data show that the 2 current levels differ in radiance by a few percent for MAS channels 2 and 3 but probably less than 1% for the longer wavelength channels. To avoid this problem altogether during future calibrations, hardware to regulate the 20-inch hemisphere current level at a fixed value is on order.

Table 1. Percent change in radiance with distance from the MAS to the Ames 20-inch integrating hemisphere.

Distance	Ch. 2	Ch. 3	Ch. 4	Ch. 5	Ch. 6	Ch. 7
0"	14.41	14.66	23.88	16.95	20.17	25.00
2"	9.91	10.34	15.67	11.02	14.29	16.67
4"	9.01	8.62	12.69	8.47	11.76	12.96
8"	6.31	6.03	8.96	5.93	8.40	8.33
14"	4.50	4.31	5.97	4.24	5.88	4.63
20"	3.60	3.45	3.73	2.54	4.20	2.78
28"	1.80	2.59	2.24	1.69	2.52	1.85

Another issue pursued during the past six months was the characterization of all 50 spectral channels of the MAS. The MAS was shipped to Stennis Space Center where spectral calibrations of all channels were performed on 17-19 August. After analyses of these data and discussion between GSFC and Ames engineers it was decided that the Stennis spectral characterization was preferred over comparable measurements performed at Dædalus Enterprises. Calibration sensitivity studies of the effects of gaseous absorption on integrating sphere output were conducted by Steve Platnick using Monte Carlo simulation of the photon path length distribution within the sphere. MAS measurements are needed to compare with these model simulations.

The 50-Channel Data Acquisition/Digitizer System (DAS) is now a complete part of the data system for the MAS. It is housed in an enclosure inside the System Box along with a host Ampro Computer Board and an Exabyte Tape Drive. The DAS was developed at the Space Sciences Laboratory at UC Berkeley and built by Berkeley Camera Engineering. Upon completion of the DAS, each channel has digital control of the input gain with a second stage gain and offset to guarantee optimal ADC performance, and consists of the following features: (1) a low noise instrumentation amplifier with selectable gains of 1, 10 and 100 via digitally controlled relays, (2) a second instrumentation amp that has digitally controlled gains of 1, 10, 100 and 1000, and an offset adjustment, (3) a two-channel, 16-bit, 100 kHz A/D Sample/Hold Converter configured for a bipolar analog input and a 2nd compliment digital output in Synchronous Self-Clocking Mode for optimum performance with  $4\times$  oversampling to reduce aliasing from system noise while eliminating ringing effects seen in all analog filters, and (4) an on-board voltage regulation. There are seven hours allocated for test flights (3-5 January 1995) to fine tune the onboard software.

Post-flight CAR calibrations for the MAST (Monterey Area Ship Tracks) experiment, based in Monterey, CA during June 1994, were completed on September 7. Subsequent to this calibration, all optics of the CAR were cleaned and recalibrated prior to the SCAR-C (Smoke, Clouds And Radiation-California) experiment. Analyses of these data are currently underway. Some localized anomalies of CAR radiance were observed due to a quick change in manual gain during a scan cycle. Max Strange is looking into an addition of a small circuit board to the panel box to synchronize the gain change within the scan cycle that will improve data collection.

*c. MODIS-related Services*

*BOREAS experiment*

The MAS participated in the BOREAS campaign (Boreal Ecosystem-Atmosphere Study, based in Prince Albert, Saskatchewan and Thompson, Manitoba during July-August 1994) for four flights (July 21 and 24, August 4 and 8). Twelve MAS bands were selected and centered at 0.547, 0.664, 0.745, 0.786, 0.834, 0.875, 0.945, 1.623, 2.142, 3.90, 11.002 and 12.032  $\mu\text{m}$  with 8-bit resolution. The absolute visible and near-infrared calibrations for BOREAS were derived by Ames from the pre- and post-flight calibration over the Ames 30-inch sphere source. A conference call was conducted between Goddard and Ames to discuss MAS spectral calibration and the results obtained from the Stennis and Dædalus spectral characterization experiments. Stennis spectral calibration measurements were selected for MAST data processing. Finally, all five calibration runs were processed by Tom Arnold, with the resulting calibration coefficients passed on to Ken Brown.

*SCAR-C experiment*

Both MAS and CAR participated in the SCAR-C field experiment (Smoke, Clouds and Radiation-California; September 21 - October 4, 1994). The SCAR-C MAS configuration was as follows: 0.547, 0.664, 0.875  $\mu\text{m}$  at 0.8 reflectance saturation ( $R$ ), two 1.623  $\mu\text{m}$  bands at high (786 K/2.0  $R$ ) and low (650 K/0.2  $R$ ) gain settings, 1.88  $\mu\text{m}$  (0.2  $R$ ), 2.142  $\mu\text{m}$  (580 K/0.83  $R$ ), two 3.90  $\mu\text{m}$  bands at low (330 K/0.39  $R$ ) and high (500 K/28.5  $R$ ) gain settings, and two regular thermal channels at 11.002 and 12.032  $\mu\text{m}$ . The CAR spectral bands were selected at 0.47, 0.67, 0.87, 1.03, 1.27, 1.22, 1.55, 1.64, 1.72, 2.10, 2.20, and 2.30  $\mu\text{m}$ . Both MAS and CAR operated for about 30 flight hours. Three coordinated measurements of the ER-2 and C-131A over smoke plumes, prescribed forest burns, and wildfires were obtained on 21 and 27 September. Both MAS and CAR data processing are currently underway.

*The first ADEOS symposium/workshop*

The first International ADEOS (Advanced Earth Observing Satellite) Symposium was held in Kyoto, Japan on 6-9 December 1994. The ADEOS will be launched by the Japanese H-II rocket from Tanegashima Space Center in February 1996

and is equipped with eight sensors for marine, coastal, land, and atmospheric observations. Three of the eight ADEOS sensors are of immediate interest to MAS and CAR research activities. These sensors are (i) Ocean Color and Temperature Scanner (OCTS,  $\pm 40^\circ$  cross-track with  $\pm 20^\circ$  tilting capability) with 12 bands centered at 0.412, 0.443, 0.490, 0.520, 0.565, 0.665, 0.765, 0.865, 3.715, 8.525, 10.85, and 11.95  $\mu\text{m}$  ( $\sim 700$  m resolution at nadir); (ii) Advanced Visible and Near-Infrared Radiometer (AVNIR,  $\pm 40^\circ$  cross-track) with 4 multispectral bands centered at 0.460, 0.560, 0.650, and 0.825  $\mu\text{m}$  ( $\sim 16$  m resolution) with one panchromatic band at 0.52-0.68  $\mu\text{m}$  ( $\sim 8$  m resolution); and (iii) Polarization and Directionality of Earth's Reflectances (POLDER,  $114^\circ$  wide-field-of-view imaging radiometer/polarimeter) with 8 bands centered at 0.443, 0.490, 0.565, 0.665, 0.763, 0.765, 0.865, and 0.910  $\mu\text{m}$  (0.443, 0.665, and 0.865  $\mu\text{m}$  with additional polarization measurements). In the upcoming FIRE-III Arctic experiment, it will be very beneficial for the NASA ER-2 and University of Washington C-131A aircraft to coordinate with ADEOS overpass times to obtain simultaneous measurements using MAS and CAR.

### *Meetings*

1. Michael King attended the BOREAS, experiment in Saskatchewan and Manitoba, Canada, a SCAR-B workshop in Brasilia, Brazil, and the EOS Payload Panel meeting in Landover, MD.

2. Michael King attended the EOS Science Executive Committee (SEC) meeting in Chicago, IL.

3. Michael King, Si-Chee Tsay and Steve Platnick attended the 1st International Airborne Imaging Spectrometer Calibration Workshop, Strasbourg, France on 11 September 1994.

4. Michael King, Si-Chee Tsay and Steve Platnick attended the 1st International Airborne Remote Sensing Conference and Exhibition, Strasbourg, France on 12-15 September 1994 and M. D. King presented a paper entitled "MODIS Airborne Simulator: Status, calibration, and Earth remote sensing applications."

5. Menghua Wang attended the MODIS test data workshop at Polson, MT on 20-22 September 1994 to report on activities related to the MODIS cloud retrieval algorithms developed by the Cloud Retrieval Group.

6. Si-Chee Tsay attended the 2nd International Conference on Air-Sea Interaction and on Meteorology and Oceanography of the Coastal Zone, Lisbon, Portugal on 22-27 September 1994 and presented a paper entitled "Remote sensing and in-situ measurements of cloud radiative and microphysical properties in ASTEX."

7. Steven Platnick attended the European Symposium on Satellite Remote

Sensing, Rome, Italy on 26-30 September 1994 and presented a paper entitled "Status and calibration of the MODIS Airborne Simulator for Earth remote sensing applications."

8. Michael King, Tom Arnold, Dave Augustine, Ken Brown, Ted Hildum, Ward Meyer, Steve Platnick, Skip Reber, Si-Chee Tsay and Menghua Wang attended a one-day workshop (5 October) held at the National Institute of Standards and Technology, hosted by Carol Johnson, to discuss calibration issues.

9. Michael D. King, Steve Platnick, Si-Chee Tsay and Menghua Wang attended the MODIS Science Team meeting in Greenbelt, MD on 12-14 October 1994 and discussed revisions to their ATBD (Algorithm Theoretical Basis Document), in response to comments from reviewers.

10. Michael King attended and made presentations at the EOS Investigators Working Group (IWG) meeting and evening SEC meeting in Hunt Valley, Baltimore, MD on 19-21 October 1994.

11. Michael King, Steve Platnick, Si-Chee Tsay and Menghua Wang attended the SCAR-B Science Planning meeting and SCAR-C science workshop at Goddard, Greenbelt, MD on 29 November 1994.

12. Michael King, Si-Chee Tsay and Menghua Wang attended the CERES Science Team meeting in Williamsburg, VA on 30 November-2 December 1994 and discussed collaboration between the MODIS and CERES science teams on cloud retrieval algorithms.

13. Si-Chee Tsay attended the first ADEOS symposium/workshop and the TRMM meeting in Kyoto, Japan on 6-9 December 1994 and presented recent research activities using MAS and CAR measurements, considered to be of interest to the ADEOS community.

14. Michael King and Steve Platnick attended the MAST workshop in Monterey, CA on 12-15 December 1994 and presented preliminary results from MAS cloud retrievals.

#### *Seminar*

1. Michael King gave a dinner banquet address entitled "Earth Observing System (EOS): Science Objectives and Challenges" to the Potomac Geophysical Society at the Fort Meyers Officers Club, Arlington, VA, on 17 November 1994.

### III. Data/Analysis/Interpretation

#### a. *Data Processing*

The MAS 50-channel quick view system was developed using IDL by Dave Augustine and Liam Gumley and used to review all MAS data from TOGA COARE and CEPEX to find likely candidate flights for visible/near-IR in-flight calibration. Timing tests for a less ambitious quick view program (using only IDL graphics, with no Widgets) did show that it runs fast enough to keep up with the data volume (about 5.5 times the data acquisition speed). However, the speed is really limited by the rate of transferring data from the Exabyte tape (~500 kb/sec), and hence the 50 channel (57344 bytes) quicklook system could only run at about 1.5 times the data acquisition speed. Thus, it was decided that a large hard disk be used in the field to dump the tape data after each MAS flight. The data on the hard disk would then be used in conjunction with the quicklook system to provide acceptable viewing speed.

Liam Gumley developed a way to display MAS images on a map base in a standard map projection for a quick overview of an entire ER-2 mission. The science quick looks generated during Level-1B MAS processing were used instead of Level-1B radiance data for speed. Navigation data for each pixel in the quicklook images were computed using the start and end points of the flight line derived from the flight summary file. The images were sized to provide adequate detail, without consuming too much memory during gridding. All quicklook images from FIRE-II, ASTEX, SCAR-A, and MAST have been processed to produce flight line mosaic images for all flights in these missions. In future missions, this will become part of the Level-1B processing sequence. In addition, Jason Li (a new member of the Cloud Retrieval Group who replaced Liam Gumley on 21 November) developed methods for plotting C-131A flight tracks over MAS imagery and for automating the mosaic GIF image for an arbitrary MAS channel. Examples of MAS imagery for 0.664 and 3.725  $\mu\text{m}$  on 29 June 1994 during MAST are shown in Figs. 3 and 4, respectively. The MAS World Wide Web home page was established by Liam Gumley and accessed over 680 times during July and August (not including sub pages, and accesses from our own 'redback' workstation).

Tom Arnold completed a report detailing how the calibration should be adjusted for each TOGA/COARE flight based on pre-flight relative calibrations using a dual lamp light box. The adjustment algorithm for CEPEX was based on a linear extrapolation of the final TOGA/COARE light box calibration, and the post-flight calibration of the MAS as determined from measurements of the Ames 30-inch sphere. These calibration coefficients were used by Paul Hubanks to complete the MAS Level-1B data processing for the TOGA/COARE mission and the CEPEX data processing is currently underway.

b. *Analysis and Interpretation*

The entire MAS ASTEX data set was processed by Menghua Wang for 42 cloudy flight lines. Three output files were generated for each flight line: (i) retrieved cloud optical thickness ( $\tau_c$ ), (ii) effective particle radius ( $r_e$ ), an average of our two-channel (0.664 and 2.142  $\mu\text{m}$ ) and three-channel (0.664, 1.621, and 2.142  $\mu\text{m}$ ) algorithm retrievals, and (iii) %-difference of the retrieved effective particle radius for these two methods. The results for the %-difference represent the retrieval accuracy (both spectral/radiometric calibration and aerosol/ice cloud contamination), since theoretically for plane-parallel water clouds the retrieved effective particle radius using these two different methods should yield the same value. On the other hand, the %-difference may be viewed as an indication of the effect of cloud inhomogeneity. The retrieved cloud optical thickness and effective radius for ASTEX are presented as marginal and joint probability density functions for statistical interpretation and for the purpose of comparing these retrievals with *in situ* microphysical measurements. The corresponding microphysical data that we examined from the University of Washington's C-131A research aircraft include radar altitude, condensation nuclei, droplet concentration, liquid water content and effective particle radius from the PVM, FSSP and OAP probes. These results were presented at the Lisbon Conference during the ASTEX special session. In general, the statistical properties of the MAS-retrieved effective radius are in reasonable agreement with *in situ* measurements. Similar results were obtained by Steve Platnick by comparing AVHRR 3.75  $\mu\text{m}$  retrievals with corresponding *in situ* microphysical measurements.

In the process of retrieving cloud properties from ASTEX data, contributions from atmospheric aerosols have been neglected. The addition of an aerosol effect on cloud retrievals will, no doubt, complicate the retrieval algorithm, due in part to the difficulty of separating the effects of aerosol scattering from those of cloud scattering. Figure 5 shows a red (2.14  $\mu\text{m}$ ), green (1.62  $\mu\text{m}$ ), blue (0.66  $\mu\text{m}$ ) composite image derived from MAS data on 17 June 1992 between 12:21:21 and 12:27:33 UTC. In this image, the ER-2 aircraft was flying from top to bottom down the center of the image, with a heading of  $304^\circ$  and the MAS scanning clockwise. This image was remapped to a horizontal grid at 1 km altitude, thus providing a uniform spatial scale over the  $72 \times 36$  km size of the image. Striking features shown in Fig. 5 include a boundary-like broken cloud (running from upper-left to lower-right) that separates a clean cloud scene at the upper-right corner and a dirty cloud scene with a haze layer aloft (very dense at lower-right corner). Aerosols are expected to have strong backscattering in the shortwave range (or blue color at lower-right). This perturbation in reflected visible radiance by aerosols immediately affects the retrieval of cloud optical thickness and, in turn, the retrieved particle radius.

Also shown in Fig. 5 is the flight track of the University of Washington C-131A aircraft, indicated as a red dashed line from the upper-left to the lower-right of this image. The C-131A was flying at an altitude of 1160-1120 m within the

cloud. Scattergrams of measured cloud effective radius, droplet concentration, and liquid water content (with a threshold value of  $0.05 \text{ g m}^{-3}$ ) are shown in Fig. 6 for the C-131A transect. As shown in Fig. 6a, the effective radius increases by about  $6 \text{ }\mu\text{m}$  (and the liquid water content by about  $0.5 \text{ g m}^{-3}$ ) as the aircraft moves westward across the microphysical transition. The liquid water content shown in Fig. 6c becomes out-of-phase with the effective radius shown in Fig. 6b as the aircraft crosses  $23.7^\circ\text{W}$ . In addition, the droplet concentration is in-phase with the liquid water content. It is more likely that the western portion of the area flown by the C-131A was heavily influenced by continental air and that the transition boundary noted in the MAS image and measured *in situ* by the C-131A was meteorological and not microphysical.

The indirect effect of aerosols on cloud properties was studied during MAST. On 29 June 1994, the NASA ER-2 aircraft overflowed a ship track produced by a dedicated Navy ship on flight line 7. Figure 7 shows the retrieval of cloud optical thickness (Fig. 7a) and effective radius (Fig. 7b) for one scan line across the ship track (pixel location 400-480 in these figures). In the optical thickness figure, separate curves denote the results of the optical thickness retrieval obtained using a two channel algorithm ( $0.664 \text{ }\mu\text{m}$  plus the channel indicated in the figure legend). Since most of the optical thickness information arises from the visible channel ( $0.664 \text{ }\mu\text{m}$  in this case), it is not surprising that all retrievals gave nearly the same results for  $\tau_c$ . Of perhaps greater interest is the fact that none of the retrievals suggested much of an optical thickness enhancement in the region of the ship track.

Figure 7b shows a corresponding retrieval (again using two channels) for the effective radius. For this parameter, in contrast to Fig. 7a, the resulting retrieval for  $r_e$  was a function of the channel that was used in the retrieval. The  $3.725 \text{ }\mu\text{m}$  retrieval, which required an adjustment for atmospheric emission, yielded the largest effective radii. The  $1.623$  and  $2.142 \text{ }\mu\text{m}$  retrievals were more nearly the same, with the  $2.142 \text{ }\mu\text{m}$ -derived effective radius showing a somewhat larger dynamic range than the  $1.623 \text{ }\mu\text{m}$  retrieval. The fact that these retrievals were all different raises a number of questions, such as the accuracy of the thermal corrections in the  $3.725 \text{ }\mu\text{m}$  retrieval and the accuracy of the refractive indices for water at all wavelengths. This figure is exceedingly valuable, for it shows, for the first time, the simultaneous retrieval of optical thickness and effective radius using all three near-infrared channels that will be available on MODIS, channels that are not currently available on any spacecraft sensor.

Figure 8 shows the marginal probability density function of optical thickness (Fig. 8a) and effective radius (Fig. 8b) for selected regions inside (dotted) and outside (solid) the ship track illustrated in Fig. 7. As was the case in Fig. 7a, there is no apparent difference in the optical thickness inside and outside a ship track (Fig. 8a), whereas the effective radius is considerably larger outside the ship track than inside (Fig. 8b). The optical thickness and effective radius retrievals shown in Fig. 8 are the result of the  $0.664$  and  $2.142 \text{ }\mu\text{m}$  retrieval algorithm.

#### IV. Anticipated Future Actions

- a. Complete the analyses of FIRE-II Cirrus and ASTEX data gathered by the MAS and CLS, as well as theoretical studies, and submit manuscripts to journals.
- b. Process and further analyze MAS and in situ microphysical data obtained from the MAST field campaign and prepare manuscript for submission to journal.
- c. Compare retrieved cloud parameters from the 3.75  $\mu\text{m}$  channel with those obtained from the 0.665, 1.623 and 2.142  $\mu\text{m}$  channels, and look into the spectral signature of vertical profile in effective particle radius.
- d. Conduct sensitivity study of aerosol effects on retrieved optical thickness and effective particle radius, based on CAR measurements obtained during the Kuwait Oil Fire and SCAR-A experiments.
- e. Continue to analyze surface bidirectional reflectance measurements obtained during the Kuwait Oil Fire, LEADDEX, ASTEX and SCAR-A experiments.
- f. Attend FIRE-III Science Team Meeting and prepare for the upcoming MODIS Atmosphere Science Team activity to study Arctic stratus clouds during June 1995.
- g. Attend the Chapman Conference on Biomass Burning and SCAR-B Science Team meetings in Williamsburg, VA to further define the SCAR-B experiment to be conducted in Brazil during August-September 1995.

#### V. Problems/Corrective Actions

No problems that we are aware of at this time.

#### VI. Publications

1. King, M. D., S. C. Tsay, S. E. Platnick and M. Wang, 1994: Cloud retrieval algorithms for MODIS: Optical thickness, effective particle radius, and thermodynamic phase (version 3). MODIS Science Team, 50 pp.
2. Platnick, S. E., 1994: Photon path lengths in integrating spheres and the effect of gaseous absorption on radiance output. NASA GSFC internal report.
3. King, M. D., D. D. Herring and D. J. Diner, 1995: The Earth Observing System (EOS): A space-based program for assessing mankind's impact on the global environment. *Opt. Photon. News*, **6**, 34-39.
4. Gumley, L. E., and M. D. King, 1995: Remote Sensing of flooding in the US upper midwest during the summer of 1993. *Bull. Amer. Meteor. Soc.*, in press.

5. Wielicki, B. A., R. D. Cess, M. D. King, D. A. Randall and E. F. Harrison, 1995: Mission to Planet Earth: Role of clouds and radiation in climate. *Bull. Amer. Meteor. Soc.* (in press).
6. King, M. D., S. C. Tsay and S. E. Platnick, 1995: In situ observations of the indirect effects of aerosol on clouds. *Dahlem Workshop on Aerosol Forcing of Climate*, R. J. Charlson and J. E. Heintzenberg, Eds., John Wiley and Sons (in press).

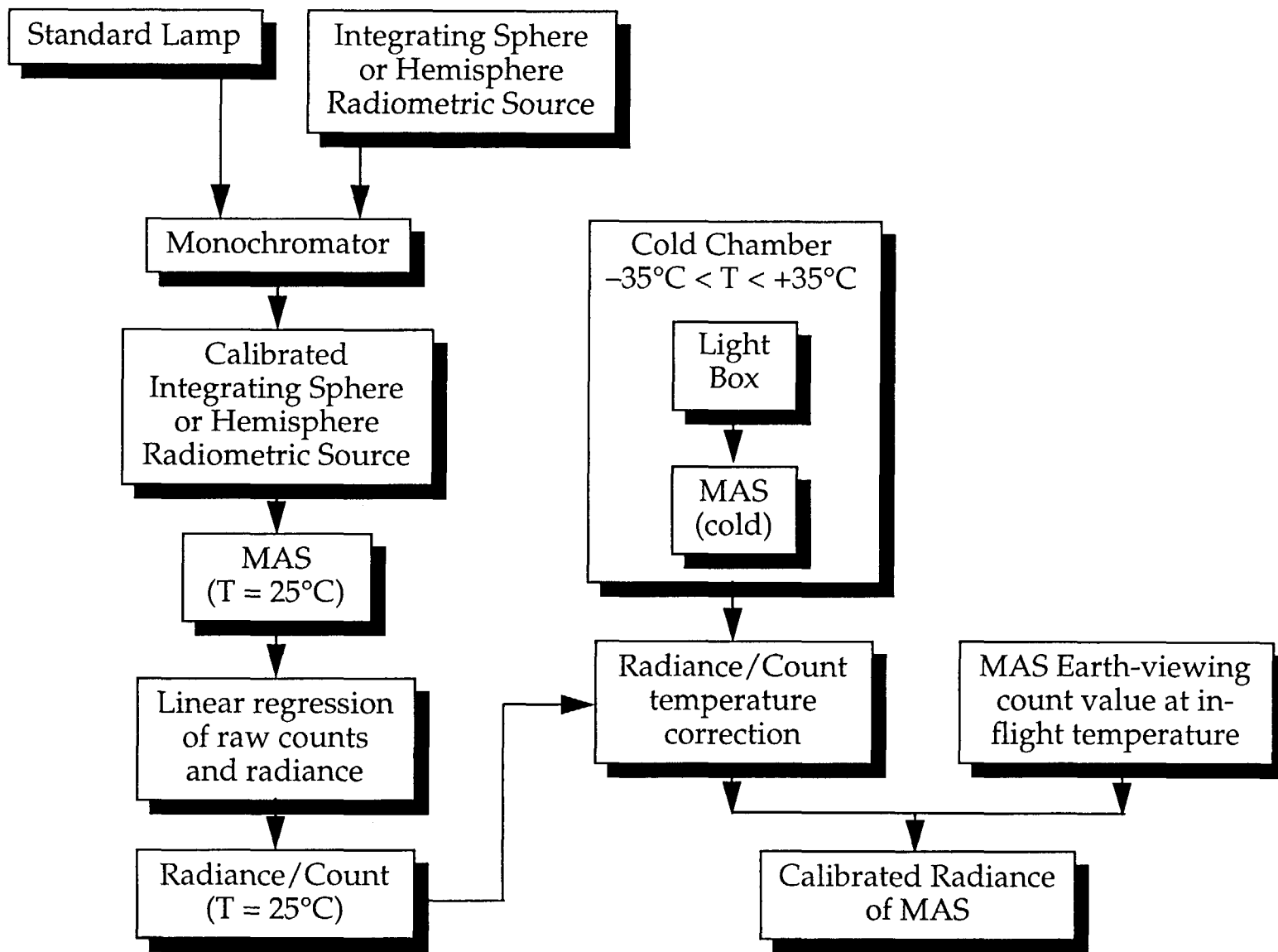


Figure 1. Schematic representation for MAS calibration procedure, including radiometric source calibration and temperature correction.

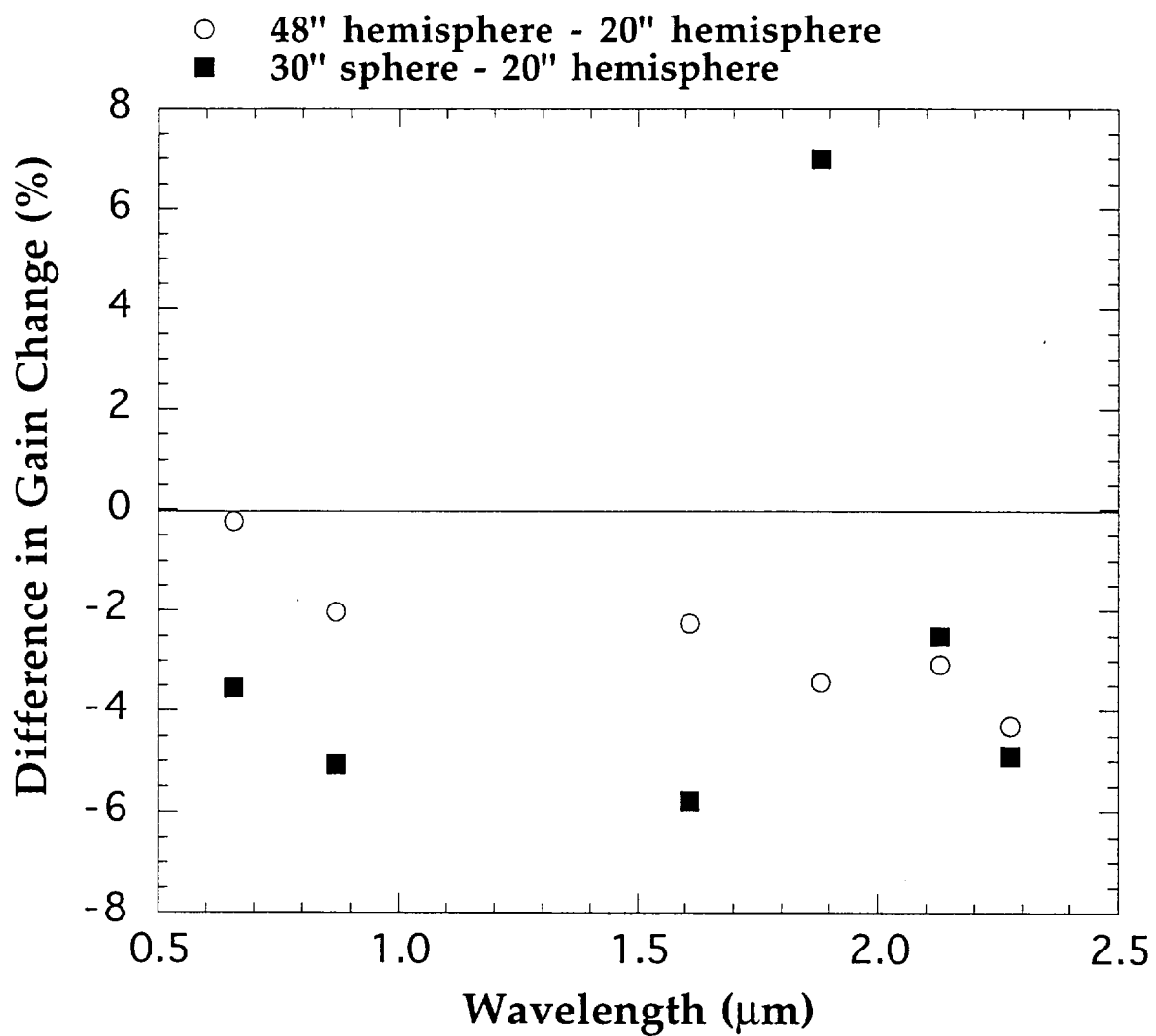


Figure 2. Comparison of Goddard 48-inch hemisphere and Ames 20-inch hemisphere and 30-inch sphere sources in gain change.

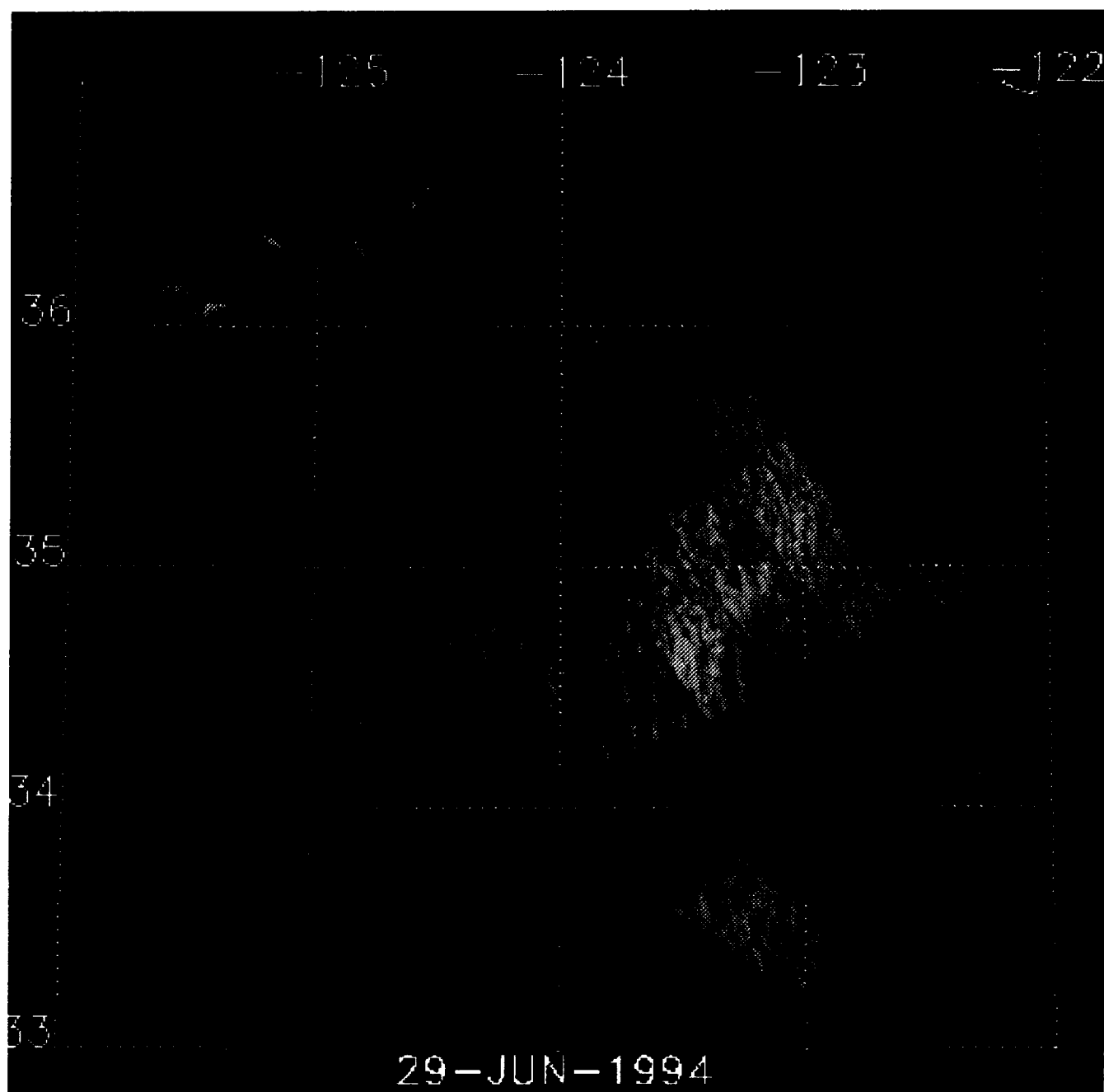


Figure 3. MAS Mosaic GIF image for visible  $0.664\ \mu\text{m}$  during MAST.

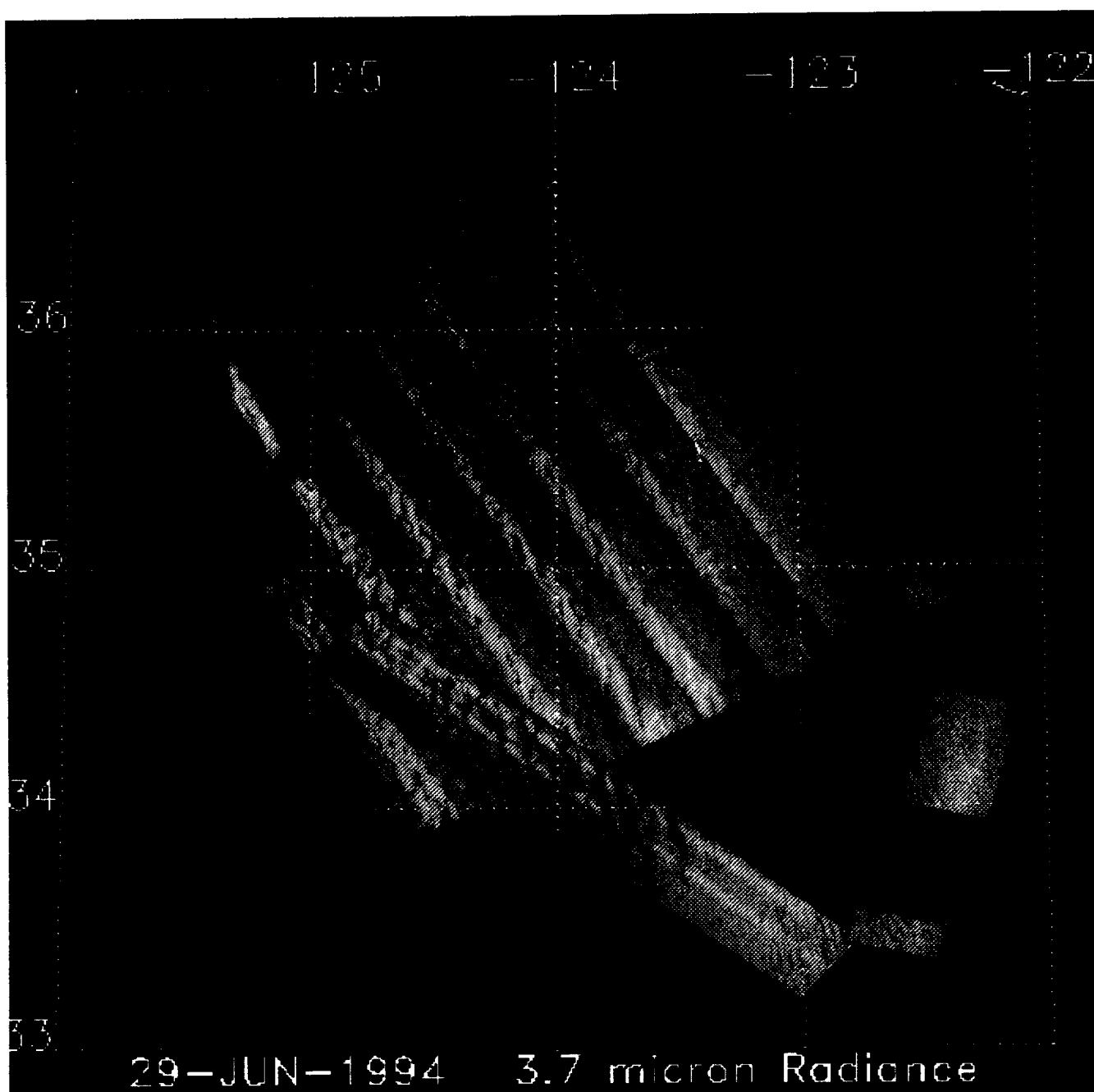


Figure 4. Same as in Fig. 3 but for 3.725  $\mu\text{m}$ .

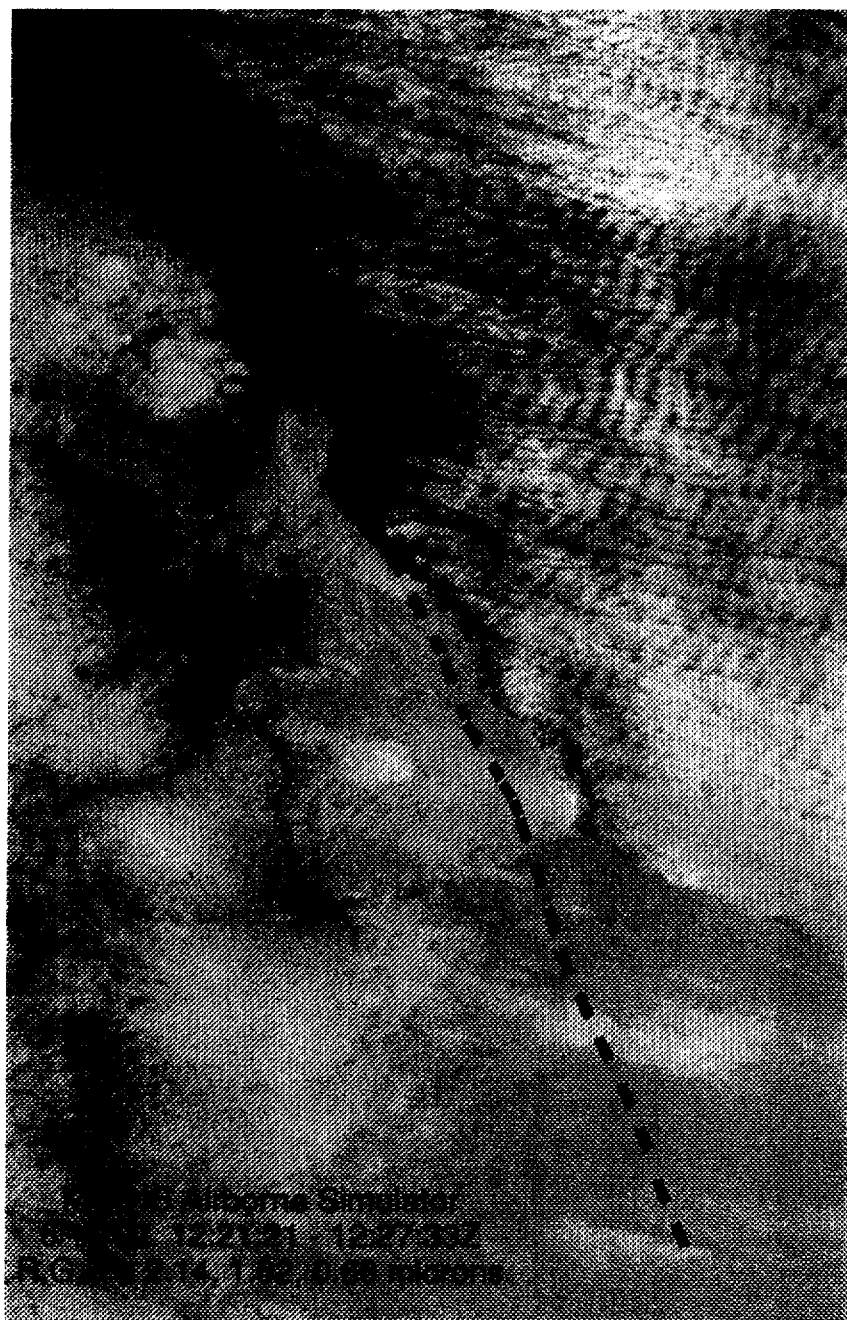


Figure 5. MAS RGB imagery during ASTEX with superimposed flight track of University of Washington C-131A.

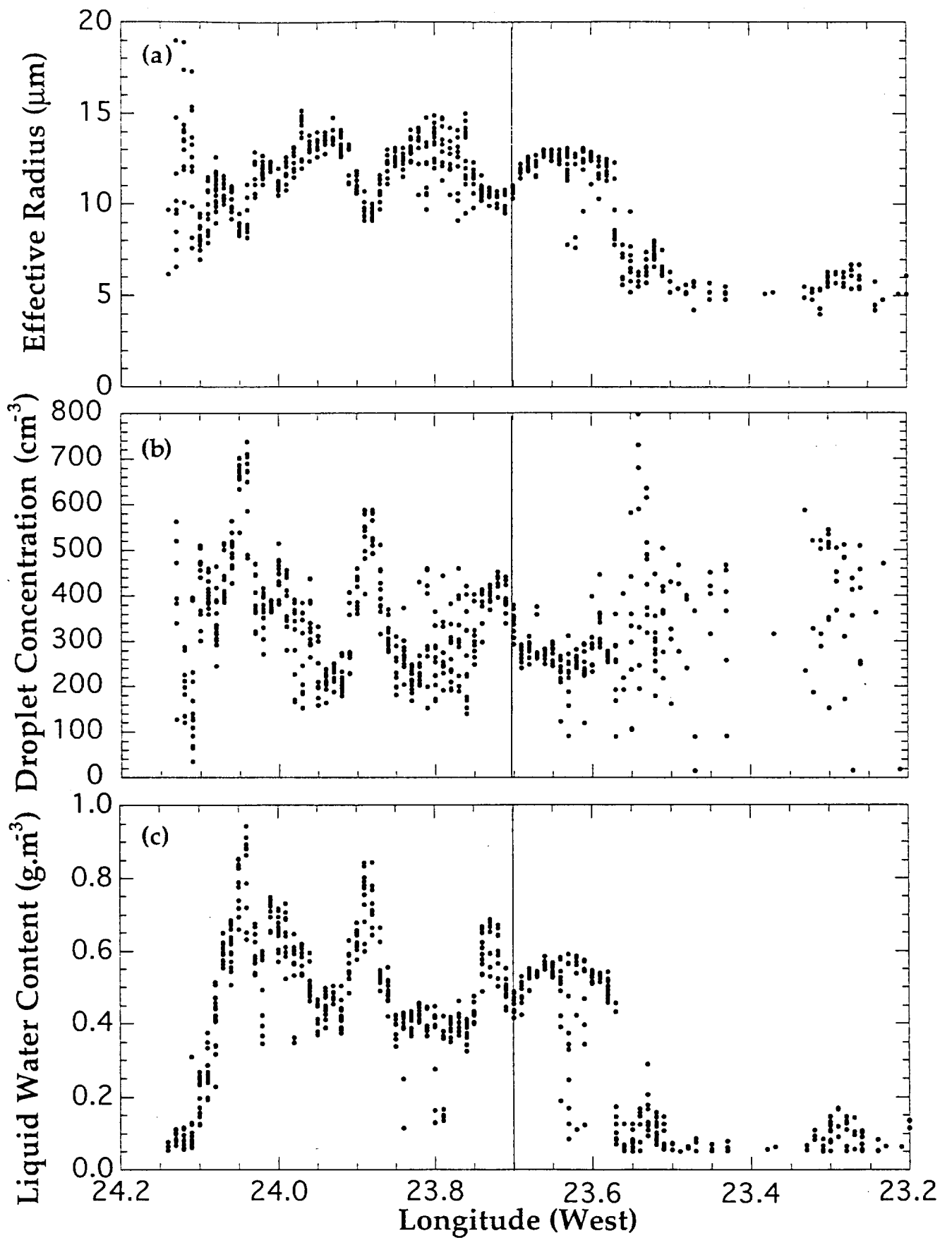


Figure 6. In situ measurements of microphysical parameters, corresponding to flight track shown in Fig. 5.

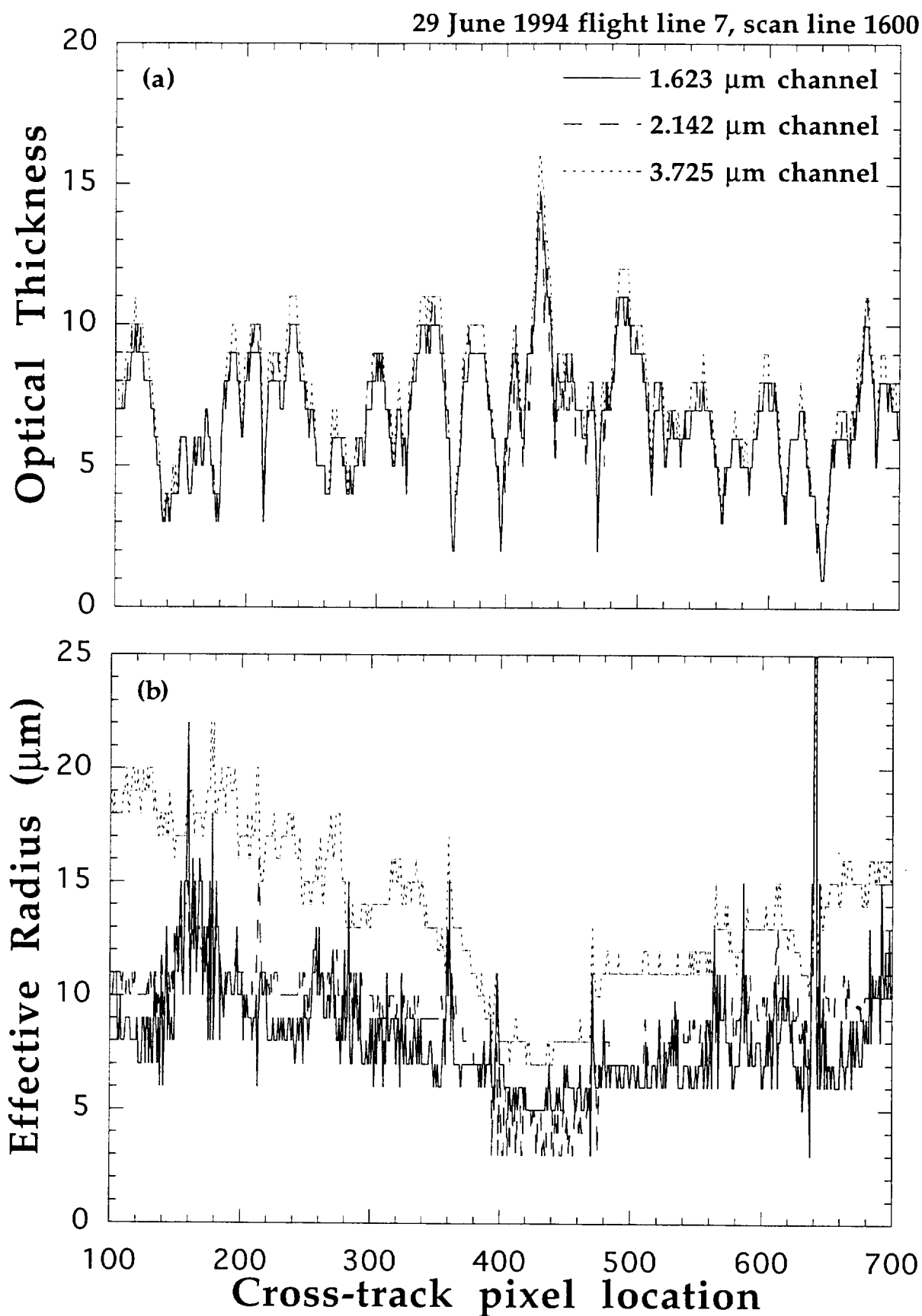


Figure 7. Retrieval of cloud properties during MAST (see text for details)

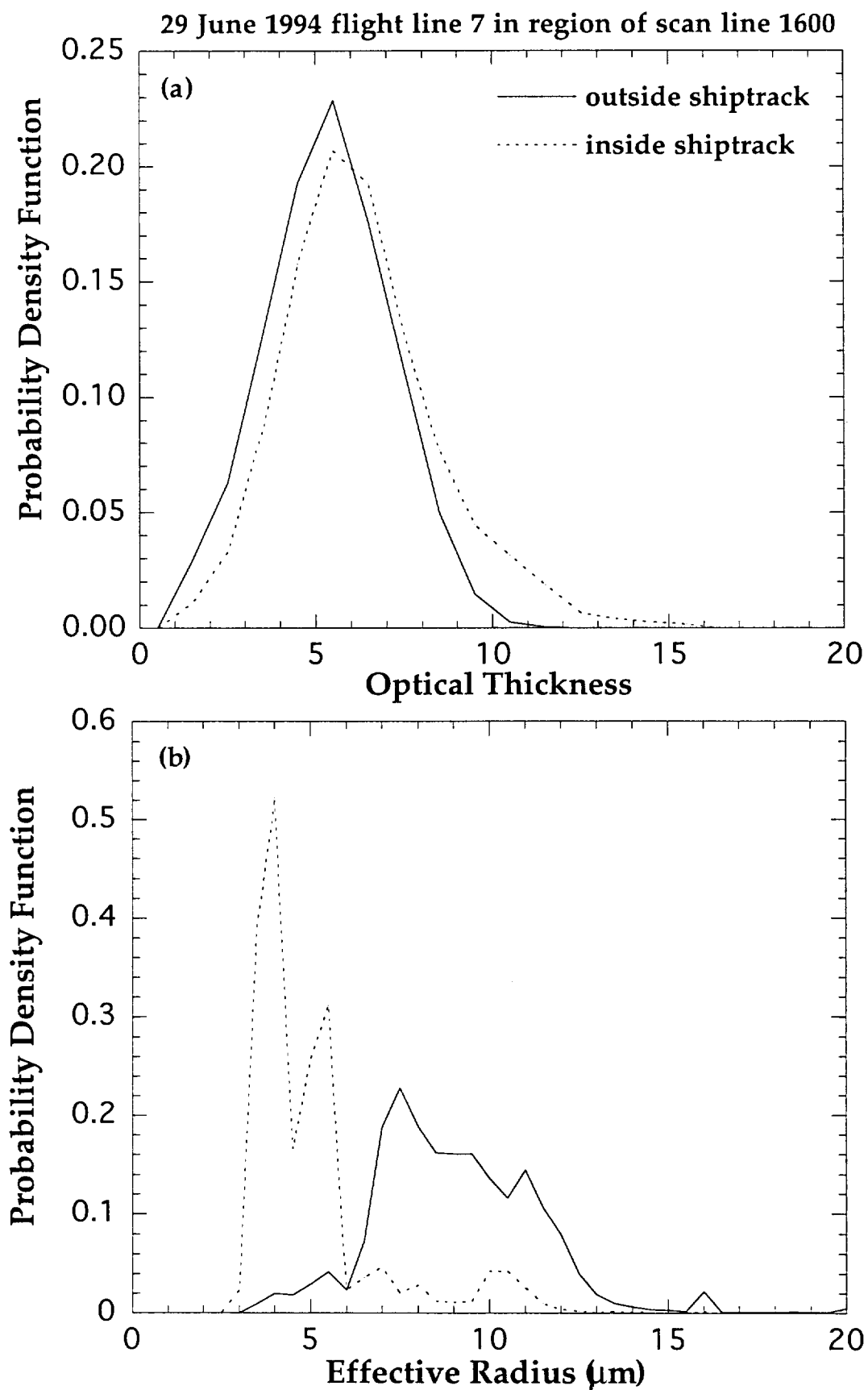


Figure 8. Statistics of retrieved cloud properties during MAST (see text for details).